Continental Shelf Research ▮ (▮▮▮▮) ▮▮▮–▮▮▮

Contents lists available at ScienceDirect

Continental Shelf Research

journal homepage: www.elsevier.com/locate/csr

Research papers

Acoustic measurement of suspended sediment concentration profiles in an oscillatory boundary layer

Francisco Pedocchi [a,*], Marcelo H. García [b,1]

[a] Instituto de Mecánica de los Fluidos e Ingeniería Ambiental, Facultad de Ingeniería, Universidad de la República, Julio Herrera y Reissig 565, CP 11300 Montevideo, Uruguay
[b] Ven Te Chow Hydrosystems Laboratory, Department of Civil and Environmental Engineering, University of Illinois at Urbana-Champaign, 205 N. Mathews Avenue, Urbana, IL 61801, USA

ARTICLE INFO

Article history:
Received 14 July 2010
Received in revised form
4 April 2011
Accepted 12 May 2011

Keywords:
Ultrasonic Velocity Profiler
Suspended sediment
Oscillatory flow

ABSTRACT

The use of an Ultrasonic Velocity Profiler (UVP) to obtain phase-averaged velocity and turbulent Reynolds stress profiles inside an oscillatory boundary layer flow is described in detail and possible error sources are summarized. Since the instrument also reports the acoustic backscatter, a novel application of the same ultrasound profilers to obtain phase-averaged suspended sediment concentration profiles and the errors involved in this technique are carefully discussed. The experiments were performed in the Large Oscillatory Water-Sediment Tunnel (LOWST), which has been a recent addition to the experimental facilities of the Ven Te Chow Hydrosystems Laboratory at the University of Illinois at Urbana-Champaign. The results showed that for the selected transducer frequency and flow, the instrument ability to characterize turbulence is compromised by the presence of Doppler noise and the size of the sampling volume. Regarding the suspended sediment estimation, it was found that the calibration obtained using water samples yielded good results, allowing for the study of the suspended sediment evolution along the oscillation.

1. Introduction

The transport of sandy sediment in suspension is particularly important in wave dominated environments. In these environments, wave action can resuspend the bed sediment, making it very easy to transport by currents that otherwise would not be able to mobilize it. The presence of bedforms increases the suspended sediment, since flow separation and vortex shedding can transport sediment up into the water column. In this note we examine the use of an acoustic Doppler profiler, the Ultrasonic Velocity Profiler (UVP) produced by Met-Flow SA, to measure both velocity and suspended sediment profiles in an oscillatory boundary layer. The UVP uses the Doppler shift between the transmitted and the received signal frequencies to compute the velocity of the reflective particles transported in the water flow. Additionally, the UVP reports the raw backscatter amplitude, which can be used to estimate the suspended sediment profile over the cycle. The theory involved in the estimation of the suspended sediment from acoustic backscatter is applied to the case of the UVP. Given the number of users of the UVP around the world we expect that this work should encourage them to extend the use of the instrument for suspended sediment measurements.

Previous applications of the UVP or similar devices for water flow measurements have been reported in the literature (e.g. Lemmin and Rolland, 1997). However, most of the measurements involved unidirectional flows over fix beds with no suspended sediment. Contrary to the case of light-based velocity measurement methods, such as Particle Image Velocimetry or Laser Doppler Anemometry, relatively large amounts of suspended sediment do not present a difficulty for doing velocity measurements with the UVP. As examples of the proposed application of the UVP, this article presents measurements obtained at the Large Oscillatory Water Sediment Tunnel (LOWST) at the University of Illinois at Urbana-Champaign. A complete description of the LOWST and its operation can be found in Pedocchi and García (2009). For these experiments the water flows over a movable sediment bed, resulting in a coupled evolution of water flow and sediment bed morphology. Due to these rapidly changing conditions, obtaining a complete velocity profile in a short amount of time is one of the most appealing characteristics of acoustic profilers for this application.

Results for a regular oscillatory boundary layer flow over the same sediment bed are presented and discussed. Unsteady flow present additional challenges regarding their measurement, since the flow unsteadiness introduces the requirement of multiple realizations in order to obtain statistically meaningful information.

* Corresponding author. Tel.: +598 2 7113386x218; fax: +598 2 7115277.
E-mail addresses: kiko@fing.edu.uy (F. Pedocchi), mhgarcia@illinois.edu (M.H. García).
[1] Tel.: +1 217 2444484; fax: +1 217 3330687.

0278-4343/$ - see front matter © 2011 Elsevier Ltd. All rights reserved.
doi:10.1016/j.csr.2011.05.013

In this sense, regular oscillatory flows present the advantage of their periodicity, and the requirement of measurements over multiple realizations and ensemble averaging is replaced by the simpler task of measuring over multiple cycles and phase averaging.

2. The Ultrasonic Velocity Profiler

A basic description of the function of the UVP is presented in this section. The UVP transducer sends a short ultrasonic pulse into the water column and as soon as it ends transmitting it starts receiving the echos returning from the reflecting particles found along the acoustic path. The time delay δt between the emission of the pulse and reception of the echos from a region located a distance r from the transducer is

$$\delta t = \frac{2r}{c}, \tag{1}$$

with c the sound speed of the transmitting medium (see Eq. (A.1) in Appendix A).

If the particles in the volume from which the sound is being scattered are moving with a velocity u_r along the axis of sound transmission, the backscattered sound will present a Doppler shift of the frequency with respect to the original frequency when measured at the transducer. Since the frequency is shifted twice, first when it hits the particle and again when it is reflected, the relation between the measured Doppler shift F_D and the velocity of the particles in the measuring volume is given by

$$u_r = \frac{F_D}{2}\lambda, \tag{2}$$

where λ is the wavelength of the ultrasound. Note that $\lambda = c/F$ and F is the emitted ultrasound frequency. The details of the Doppler shift determination can be found in the work of Lhermitte and Serafin (1984) and Lhermitte and Lemmin (1994). The UVP measures the time delay δt and the Doppler shift F_D; from them the UVP computes the component of the particle velocities inside of the measuring volumes at the different positions along the sound axis. If the measuring volume is small enough and the reflecting particles are assumed to follow the liquid motion, the projection of the liquid flow velocity u_r along the sound axis can be computed.

The maximum measurable distance from the transducer $r_{\max}$ is given by the time that the transducer is listening for echoes after a sound pulse has been emitted. This time is equal to the time between pulses, and is expressed by the pulse repetition frequency F_S. Therefore

$$r_{\max} = \frac{c}{2F_S}. \tag{3}$$

The maximum measurable velocity is given by the Nyquist sampling criteria, the maximum measurable Doppler shift is limited to one half of the pulse repetition frequency ($F_D = F_S/2$). Then, the maximum velocity along the sound beam axis $u_{r\ \max}$ that can be measured is

$$u_{r\ \max} = c\frac{F_S}{4F}. \tag{4}$$

From Eqs. (3) and (4) it can be found that

$$u_{r\ \max} r_{\max} = \frac{c^2}{8F}; \tag{5}$$

therefore, the $u_{r\ \max} r_{\max}$ product is a constant for a given sound frequency and medium. This introduces constraints on which sensor frequency should be used for different applications. For example, for the experiments in the Large Oscillatory Water Sediment Tunnel it was necessary to select 1 MHz transducers to cover the 0.5 m of water depth and maximum velocities of up to 1 m/s, placing the sensors at 30° with the vertical.

3. Velocity profiles

3.1. Computation of velocity profiles

As explained in the previous section, the UVP transducer measures the radial velocity along the sound path. If the user wants to measure the horizontal velocity across a channel type flow, it will be necessary to make some assumptions about the flow characteristics and to orient the sensor at an appropriate angle with respect to the mean flow.

The mean turbulent fluctuations ($\overline{u'^2}$, $\overline{v'^2}$, $\overline{u'v'}$), together with the mean flow horizontal $\overline{u}$ and vertical $\overline{v}$ components, can be obtained using three sensors as described by Lhermitte and Lemmin (1994). In this configuration, shown in Fig. 1, the only restriction is that the velocity field is uniform in the longitudinal direction over the region covered by the sensors. This hypothesis is hardly verified under the presence of bedforms; however, the convergent configuration of the ultrasound beams helps to improve this uniformity hypothesis especially at the point of intersection. The heterogeneity introduced by the bedforms is particularly noticeable close to the bed, and it is expected that it would decrease as we move away from it. Therefore, the convergent configuration assures that the horizontal distance between the measuring points of each sensor becomes smaller as the horizontal heterogeneity generated by the bedforms increases.

If u_{r1}, u_{r2}, and u_{r3} are the instantaneous radial velocities measured by each of the three sensors, they can be computed as a function of the horizontal and vertical velocities along each sensor sound path, (u_1, v_1), (u_2, v_2), and (u_1, v_1), as follows:

$$u_{r1} = u_1 \sin\alpha - v_1 \cos\alpha, \tag{6}$$

$$u_{r2} = -v_2, \tag{7}$$

$$u_{r3} = -u_3 \sin\alpha - v_3 \cos\alpha. \tag{8}$$

Then adding and subtracting Eqs. (6) and (8) yields

$$u_{r1} + u_{r3} = (u_1 - u_3)\sin\alpha - (v_1 + v_3)\cos\alpha, \tag{9}$$

$$u_{r1} - u_{r3} = (u_1 + u_3)\sin\alpha - (v_1 - v_3)\cos\alpha. \tag{10}$$

Averaging over several realizations and assuming that the flow is statistically uniform over the longitudinal direction (i.e. $\overline{u_1} = \overline{u_3} = \overline{u}$ and $\overline{v_1} = \overline{v_2} = \overline{v_3} = \overline{v}$) then

$$\overline{v} = -\frac{\overline{u_{r1}} + \overline{u_{r3}}}{2\cos\alpha} = -\overline{u_{r2}}, \tag{11}$$

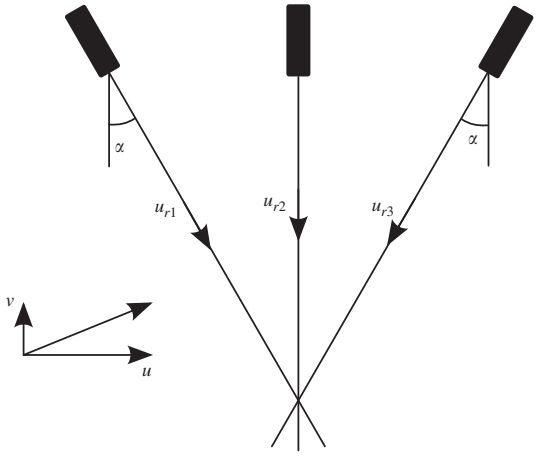

Fig. 1. Configuration of the three UVP sensors installed in the LOWST. The angle α was selected equal to 30°.

Please cite this article as: Pedocchi, F., García, M.H., Acoustic measurement of suspended sediment concentration profiles in an oscillatory boundary layer. Continental Shelf Research (2011), doi:10.1016/j.csr.2011.05.013

$$\overline{u} = \frac{\overline{u_{r1}} - \overline{u_{r3}}}{2\sin\alpha}. \tag{12}$$

To obtain statistical characterization of the flow turbulence, the fluctuations around the mean of Eqs. (6)–(8) can be squared to give

$$u_{r1}'^2 = u_1'^2 \sin^2\alpha + v_1'^2 \cos^2\alpha - 2u_1'v_1'\cos\alpha\sin\alpha, \tag{13}$$

$$u_{r2}'^2 = v_2'^2, \tag{14}$$

$$u_{r3}'^2 = -u_3'^2 \sin^2\alpha + v_3'^2 \cos^2\alpha + 2u_1'v_1'\cos\alpha\sin\alpha. \tag{15}$$

Subtracting Eq. (13) from Eq. (15) yields

$$u_{r3}'^2 - u_{r1}'^2 = -(u_1'^2 - u_3'^2)\sin^2\alpha - (v_1'^2 - v_3'^2)\cos^2\alpha + 2(u_1'v_1' + u_3'v_3')\cos\alpha\sin\alpha. \tag{16}$$

Then averaging over several realizations, and assuming again that the mean values of the fluctuations do not vary over the longitudinal direction ($\overline{u_1'^2} = \overline{u_3'^2}$, $\overline{v_1'^2} = \overline{v_2'^2} = \overline{v_3'^2}$, and $\overline{u_1'v_1'} = \overline{u_3'v_3'}$) the following expression for $\overline{u'v'}$ is obtained

$$\overline{u'v'} = \frac{\overline{u_{r3}'^2} - \overline{u_{r1}'^2}}{2\sin 2\alpha}. \tag{17}$$

Additionally, the mean square value of the longitudinal fluctuations can be obtained adding Eqs. (13) and (15). Under the same assumptions used to obtain Eq. (17)

$$\overline{u'^2} = \frac{\overline{u_{r1}'^2} + \overline{u_{r3}'^2} - 2\overline{u_{r2}'^2}\cos^2\alpha}{2\sin^2\alpha}. \tag{18}$$

Note that to compute $\overline{u'^2}$ the value of $\overline{u_{r2}'^2}$ is needed; $\overline{u_{r2}'^2}$ is also needed to compute the mean square value of the vertical fluctuations,

$$\overline{v'^2} = \overline{u_{r2}'^2}. \tag{19}$$

3.2. Possible error sources

Three transducers with the same configuration described in Fig. 1 were located at the top of the LOWST pointing down toward the sand bed. The spacing between the transducers was 28 cm and the angle with the vertical for the inclined transducers was set equal to 30°. In this configuration, the ultrasound beams from the three transducers cross at 5 cm above the flat sediment bed. The selected configuration proved to be a good compromise between the longitudinal distance covered by the sound beams, and the need for adequate projection of the velocity along the beams directions and the vertical distance covered by each channel due to the spreading of the beam. Additionally, the selected angle is acceptable in terms of the introduced uncertainty on the Reynolds stresses (Tropea, 1983).

The divergence half-angle (Eq. (A.4)) for the selected 1 MHz transducer is 3.4° (Met-Flow, 2002) which gives a sampling volume with a diameter of about 6 cm close to the sediment bed. Since the ultrasound beam forms an angle with the vertical, the inclined measuring volume will cover approximately 3 cm along the vertical direction. This fact will degrade the accuracy of the measurements close to the bed where the vertical variations of the velocity are more significant. Filtering effects are also introduced by the temporal averaging that is needed in order to reduce the noise in the signal. Fast sampling is desired in order to resolve the turbulence adequately. However, higher sampling frequencies are associated with higher levels of noise. Lemmin and Rolland (1997) have shown that for most applications averaging 32 instantaneous samples is enough to determine unambiguous velocity estimates.

The capability of the UVP to measure turbulent quantities depends on the noise levels of the reported signal and the eventual filtering effects of the averaging process involved on the sampling procedure. The possible sources of noise for coherent Doppler acoustic systems have been described by Lhermitte and Lemmin (1994) and Voulgaris and Trowbridge (1998). They include errors related to the computation of the Doppler shift and errors related to the fact that the sound return is originated by scattering particles contained inside a finite sampling volume. This last source includes the effect of the random motion of the scatters and the variation of the velocity inside the sampling volume. Previous works have identified the Doppler noise as the main source of noise in coherent Doppler acoustic systems, and they have characterized it as white noise with Gaussian probability distribution (Nikora and Goring, 1998). Being white noise, the Doppler noise cannot be removed using filtering techniques.

The presence of Doppler noise tends to artificially increase the variance of the velocity measurements. This effect can be observed in the velocity power spectrum of each radial component (Fig. 2) where the Doppler noise plateau can be identified at the higher frequencies of the velocity spectra and its energy subtracted from the mean squared values of the measured radial velocities u_r. This correction does not affect the mean velocities $\overline{v}$ and $\overline{u}$ given by Eqs. (11) and (12). For the diagonal components of the Reynolds stress tensor $\overline{u'^2}$ and $\overline{v'^2}$, the Doppler noise can be significant as shown by Eqs. (18) and (19). Therefore, the noise level should be identified from the spectra, its energy computed and explicitly subtracted in Eqs. (18) and (19) (Nikora and Goring, 1998; García et al., 2005), given that a wide enough range of the turbulence is resolved. If this condition is fulfilled, the Reynolds stress $\overline{u'v'}$ should not be affected by the Doppler noise for a symmetric configuration of the transducers. Under an ideal alignment of the sensors, Eq. (17) shows that the additional variance introduced by the Doppler noise will cancel out; assuming that the Doppler noise levels are the same for both radial velocities u_{r1} and u_{r3}, the noise is uncorrelated with the true velocity signal, and enough independent samples are averaged.

Although the backscatter returns can be originated from the fine turbulent structures (Lhermitte and Lemmin, 1994), it is clear that in the experiments discussed here most of the acoustic return was originated by the sand particles in suspension. The

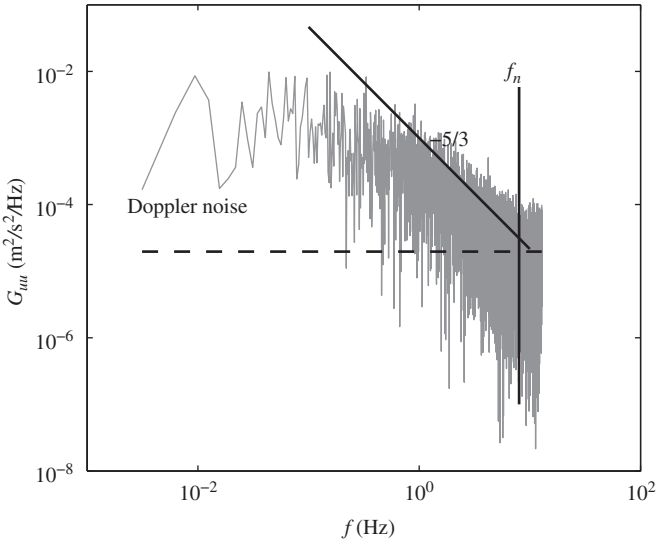

Fig. 2. Power spectrum for the vertical fluctuations recorded with the vertical transducer. The presence of Doppler noise is observed as a flattening of the spectra at the higher frequencies (above f_n). The turbulent cascade is partially observed ($-5/3$ line).

Doppler shift of these returns is used to determine the velocity by the UVP, and therefore the accuracy of the velocity measurements will be associated to the capability of the sand particles to follow the water motion. The work of Mei (1996) on the frequency response function and energy transfer function for spherical particles in a fluid is relevant in this regard. Mei (1996) defines cut-off frequencies of a particle based on the 50% energy response to the water velocity fluctuations. For sand particle with radius $a_s = 125$ μm and density $\rho_s = 2650$ kg/m^3, in water with density $\rho_w = 1000$ kg/m^3 and kinematic viscosity $\nu = 1 \times 10^{-6}$ m^2/s, the cut-off frequency would be approximately 20 Hz. The oscillation period in the experiments presented here was $T = 5$ s (0.2 Hz). Therefore, a significant range of water motions could be adequately captured from the measurement of the sand particle motions with the UVP.

4. Concentration profiles

4.1. Theoretical considerations about suspended sediment concentration estimation using ultrasound backscatter

The UVP not only reports velocity profiles, it also reports what is called the Echo Amplitude Signal. In this section the use of this signal for the estimation of the suspended sediment concentration profiles is described. If the same transducer is used for transmission and reception, the echo pressure p scattered by a single particle in clear water which is received at the transducer is (Thorne and Hanes, 2002)

$$p = \frac{a_s f p_o r_o D(\theta)^2}{2r^2} e^{i(\omega t - 2r(k - i\alpha_w))}, \tag{20}$$

where a_s is the equivalent particle radius, $f(ka_s)$ is the form function that describes the scattering properties of the particle (see Appendix A), ω and k are the angular frequency and the wave number of the sound in water ($\omega = 2\pi F$, $k = 2\pi/\lambda$, $\omega/k = c$, F and λ are the sound frequency and wavelength, respectively), p_o is the reference pressure at r_o, $D(\theta)$ is the sensor directivity which is a function of the angle with the transducer's axis θ (see Appendix A), r is the distance from the sensor, t is the time, and α_w is the sound attenuation in clear water which is a function of temperature, salinity, and sound frequency (see Appendix A).

If the sound attenuation due to the presence of other particles in suspension is considered, a generalized version of Eq. (20) is obtained

$$p = \frac{a_s f p_o r_o D(\theta)^2}{2r^2} e^{i(\omega t - 2r(k - i\alpha))}. \tag{21}$$

In the above equation, the clear water attenuation α_w in Eq. (20) was substituted by the suspension attenuation $\alpha = \alpha_w + \alpha_s$ which is the sum of the water attenuation and the sediment attenuation. The sediment attenuation can be computed as

$$\alpha_s = \frac{1}{r} \int_0^r \xi M(r)\, dr, \tag{22}$$

with $M(r)$ in kg/m^3 and ξ is the sediment attenuation constant (see Appendix A).

For a measuring volume V containing N randomly moving particles, the total pressure wave Σp measured at the transducer would be the sum of all the incoming pressure waves that have been reflected by the particles in V

$$\Sigma p = \sum_{n=1}^{N} \frac{a_s f p_o r_o D(\theta_n)^2}{2r_n^2} e^{i(\omega t - 2r_j(k - i\alpha))}. \tag{23}$$

If the total reverberation received by the transducer is the result of the sound scattered by a large number of particles in a random configuration, then the backscatter signal will be the combination of many sound waves with different amplitudes and phases. However, it would be expected that the total scattered signal Σp would be in a quite narrow frequency band. The total pressure wave Σp is a wave signal with zero mean value and mean square value $\sigma_p^2 = \langle (\Sigma p)^2 \rangle$. Under these conditions, it can be proved that the resulting pressure amplitude P of the waveform Σp is governed by the Rayleigh probability distribution (Bendat and Piersol, 2000)

$$\text{prob}(P) = \frac{P}{\sigma_p^2} \exp\left(\frac{-P^2}{2\sigma_p^2}\right). \tag{24}$$

The Rayleigh distribution of the total backscatter pressure amplitude P has been confirmed in numerous experiments in the past, and non-Rayleigh distributions are usually an indicator of not enough scatters in the sampling volume (Libicki et al., 1989).

The total acoustic intensity or square of the amplitude $P^2 = \Sigma p (\Sigma p)^*$ ($*$ denotes complex conjugate) can be shown to be dependent on the particle concentration, as follows:

$$P^2 = \Sigma p (\Sigma p)^* = \frac{(a_s f p_o r_o)^2}{4} \sum_{n=1}^{N} \sum_{m=1}^{N} \frac{D(\theta_n)^2 D(\theta_m)^2}{r_n^2 r_m^2} e^{-2ik(r_n - r_m) - 2\alpha(r_n + r_m)}. \tag{25}$$

If the particles are assumed to be randomly distributed in V, the phase of the backscattered waves from the different particles can also be assumed to be random and uniformly distributed between 0 and 2π. Furthermore, if the number of particles in the measuring volume is large enough, the cross terms in Eq. (25) would cancel out and the total acoustic intensity or mean square pressure amplitude will be given by

$$P^2 = \frac{(a_s f p_o r_o)^2}{4} \sum_{n=1}^{N} \frac{D(\theta_n)^4}{r_n^4} e^{-4\alpha r_n}. \tag{26}$$

From Eq. (26), it can be seen that the acoustic intensity will be a function of both the number of particles N and the spatial configuration of the particles inside the measuring volume "r_n". To remove the dependence on the particle spatial configuration, it is necessary to average over different realizations of the spatial configuration of the N particles.

The mean value of the acoustic intensity can be obtained averaging over realizations and converting the sum in Eq. (26) to an integral over the measuring volume, which in spherical coordinates is a hemispherical shell with thickness given by $w = n\lambda/2$, yields the following integral expression:

$$\langle P^2 \rangle = (p_o r_o f)^2 \left(\frac{3M}{16\pi a_s \rho_s}\right) \int_{r - n\lambda/4}^{r + n\lambda/4} \int_0^{\pi/2} \int_0^{2\pi} \frac{e^{-4\alpha r}}{r^2} D(\theta)^4 \sin\theta\, d\phi\, d\theta\, dr, \tag{27}$$

with n the number of cycles (or wavelengths) per pulse. The number two in the denominator of the w definition represents the fact that a pulse needs to travel twice its width for the two ends of the pulse to cover that distance. For a suspension of uniform size spherical particles, $M = 4/3\pi a_s^3 \rho_s N$ is the mass concentration, ρ_s is the particles density, and α is the suspension attenuation.

If α is relatively small and r is much larger than $n\lambda/2$, the exponential term can be moved outside the integral. Noting that the mean voltage intensity reported by the instrument $\langle V^2 \rangle$ is proportional to the mean acoustic intensity $\langle P^2 \rangle$ the following expression is obtained (Thorne and Hanes, 2002)

$$\langle V^2 \rangle = \left(\frac{K_s K_t}{r\psi}\right)^2 M e^{-4\alpha r}, \tag{28}$$

where K_s is a function of the scattering properties of the suspended sediment, K_t is a constant for the ultrasound system, and $\psi(r)$ accounts for the departure of the backscattered signal

Please cite this article as: Pedocchi, F., García, M.H., Acoustic measurement of suspended sediment concentration profiles in an oscillatory boundary layer. Continental Shelf Research (2011), doi:10.1016/j.csr.2011.05.013

from the spherical spreading in the near field (see Appendix A for a complete definition of these quantities).

4.2. Inherent uncertainty of the technique

As presented in the previous section, the amplitude of the resultant pressure signal received at the transducer is a random variable that follows the Rayleigh distribution. For a Rayleigh distribution, the mean amplitude is

$$\mu_P = \langle P \rangle = \sqrt{\frac{\pi}{2}}\sigma_p, \tag{29}$$

and the mean square amplitude is defined

$$\psi_P^2 = \langle P^2 \rangle = 2\sigma_p^2 = \frac{4}{\pi}\langle P \rangle^2, \tag{30}$$

which gives a relation between the mean square of the wave amplitude P and the variance of the waveform Σp. Finally, the amplitude variance is

$$\sigma_P^2 = \left(\frac{4-\pi}{2}\right)\sigma_p^2 = \left(\frac{4-\pi}{4}\right)\psi_P^2, \tag{31}$$

and the standard error for a measured pressure amplitude P verifies

$$\sigma_e(P) = \left(\frac{4-\pi}{4}\right)^{1/2}(\langle P^2 \rangle)^{1/2} = \left(\frac{4-\pi}{\pi}\right)^{1/2}\langle P \rangle. \tag{32}$$

Eq. (32) shows that the random configuration of the particles within the measurement volume introduces an inherent source of uncertainty into the measurements. To reduce this uncertainty, the two available options are signal integration and ensemble averaging. The first reduction is obtained as a result of the finite duration of the pressure pulse. To reduce the uncertainty by ensemble averaging, the only option is to average over multiple realizations (Libicki et al., 1989). For example, if 100 independent samples are averaged, the approximate uncertainty of P will be 5% which corresponds to 10% relative error in $\langle P^2 \rangle$ and thus in M, if the effect of the sediment on the attenuation is neglected (Thorne and Hanes, 2002). This also shows that the use of acoustic backscatter for the study of suspended sediment fluctuations is limited to low frequencies only.

Additionally, in the derivation of Eqs. (27) and (28), the concentration M (or equivalently N) was assumed to be a constant, while only the configuration of the particles inside the measuring volume was changing over the different realizations. Now, if the concentration M fluctuates, as is the case for turbulent flows, this will introduce new sources of deviation, and what it is actually obtained from averaging is a simultaneous double averaging over configurations and concentration fluctuations. This shows that deviations from the behavior predicted by Eq. (28) may be expected if the suspended sediment concentration fluctuates significantly around its mean value and the attenuation due to the sediment is large. Since the fluctuation of the sediment concentration is a function of the sediment size and the turbulence level of the flow, any calibration obtained under a particular flow condition will not necessarily apply to other flow conditions with different levels of turbulence. This has been observed to be the case when the sound attenuation is high (Hay, 1991; Admiraal and García, 2000). Finally, if the particles tend to take preferential configurations, forming clusters with length scales of the order of the acoustic waves, the cross terms in Eq. (25) will not cancel out, and they may introduce additional deviations to the suspended sediment estimations obtained from Eq. (28) (Merckelbach, 2006).

In summary, the physics of the ultrasound backscattering introduces an inherent level of uncertainty in the measurements. The user should always be aware of this, especially because of the high temporal resolution that acoustic profilers offer may encourage their use in the study of suspended sediment fluctuations. However, to obtain reliable suspended sediment concentration estimations, a number of independent samples needs to be averaged, thus limiting the foreseen high temporal resolution.

4.3. Particularities of the UVP

As mention before, the Echo Amplitude Signal which is the raw echo signal before demodulation is outputted by the UVP. The Echo Amplitude Signal is not the intensity of the echo P^2 but the echo waveform itself Σp which is an oscillating waveform (see Section 4.1). Note that most commercially available ultrasound instruments would report the sound intensity P^2. From the UVP hardware, the Echo Amplitude Signal can be obtained both as an analog signal through the "ECHO" output from the BNC rear panel using an oscilloscope or in echo dimensionless values through the UVP software. The software reports only the first echo profile for each velocity profile that is saved which is computed from the average of a certain number of measured profiles (32 is the default value).

The echo signal displayed by the UVP software is the result of passing the signal through a 14 bits ± 2.5 V AD converter ($8191 = 2.5$ V; $-8192 = -2.5$ V). It is important to know that the echo signal is amplified. The amplification of the received echo is introduced to compensate for sound attenuation by the media. The amplification is controlled by the "gain factors" ("gain start" and "gain end"), which are user-selectable in the UVP acquisition software. This is usually referred as Time Variable Gain or TVG. A gain factor of 3 roughly corresponds to an absolute gain of 1, so gain factors below 3 result in a cut-off of the digitized echo amplitude at the higher bits. However, this is of no interest for most of UVP applications in which gain factors larger than 3 are usually applied. In the UVP, the gain changes continuously without steps; therefore, the unamplified echo signal V can be obtained from the amplified V_{amp} one as

$$V = \frac{V_{amp}}{G_s}\left(\frac{G_s}{G_e}\right)^{(r-r_s)/(r_e-r_s)}, \tag{33}$$

where G_s and G_e are the start and end absolute gains, and r_s and r_e are the minimum and maximum measurable distances from the transducer, respectively. The values of the absolute gain associated with each gain factor for some of the different transducers that can be used with the UVP are shown in Table 1 (Oliver Mariette from Met-Flow, personal communication 2006).

The mean square of the amplitude $\langle V^2 \rangle$, which is needed to evaluate the suspended concentration in Eq. (28), can be obtained either by demodulating the backscatter pressure using a Hilbert transformation, computing V for each realization, squaring it, and then averaging over realizations. However, a simpler approach is possible if the Rayleigh probability distribution is assumed for V, as it was presented in Section 4.2. Therefore, the standard deviation σ_v of the raw echo signal v can be computed, and the mean square of the amplitude $\langle V^2 \rangle$ can be readily obtained from Eq. (30).

4.4. Backscatter inversion

Once the mean square amplitude profiles are known, Eq. (28) can be rearranged to give

$$M = \langle V^2 \rangle \left(\frac{\psi r}{K_s K_t}\right)^2 e^{4\alpha r} = \langle V^2 \rangle \left(\frac{\psi r}{K_s K_t}\right)^2 e^{4(\alpha_w r + \int_0^r \xi M\, dr)}. \tag{34}$$

Assuming that the system constant K_t is known from calibration, and the sediment is uniform (thus K_s is known), α_s still needs to

Please cite this article as: Pedocchi, F., García, M.H., Acoustic measurement of suspended sediment concentration profiles in an oscillatory boundary layer. Continental Shelf Research (2011), doi:10.1016/j.csr.2011.05.013

Table 1
Gain factors and absolute gains associated with them for UVP transducers with different operation frequencies. (Oliver Mariette from Met-Flow, personal communication 2006).

Gain factor	Transducer frequency (MHz)		
	0.5/1	2/4	8
3	2.17	0.91	0.65
4	4.41	1.76	1.36
5	8.82	3.41	2.80
6	16.67	6.67	5.26
7	33.33	15.00	11.11
8	60.00	25.00	23.08
9	150.00	60.00	42.86

be evaluated since it is also a function of M (Eq. (22)). Therefore, an explicit expression for M cannot be obtained, and Eq. (34) should be inverted in order to solve for M.

Several inversion methods exist in the literature (Lee and Hanes, 1995; Thorne and Hanes, 2002). In particular, Lee and Hanes (1995) presented an explicit method to invert Eq. (34) which is briefly described in Appendix B. The explicit inversion algorithm was shown to be computationally more efficient than the other approaches (Lee and Hanes, 1995), but it has the drawback that the concentration at an initial point M_I should be known from independent measurements. Nevertheless, as it is discussed in the next section, this can certainly improve the confidence on the obtained results.

5. Results and discussion

5.1. Velocity profiles

The results presented herein correspond to an experiment performed in the LOWST with the following conditions: starting from an initially flat sediment bed, the piston motion was set to have a period of 5 s and a maximum orbital velocity of 0.3 m/s inside the tunnel. The bed evolved until it reached a dynamic equilibrium state. At this point the bed was covered with three-dimensional ripples with a wavelength of about 15 cm and a height of 3 cm. The ripples were not at a fix spatial configuration but rather they slowly moved and rearranged themselves over the sediment bed. Under this bed configuration 4095 velocity profiles were acquired with each transducer, alternating transducers between each acquisition. The profiles were taken every 39 ms. The selected sampling interval and the use of a trigger to start the data acquisition assure that samples are acquired exactly at the same phase in the period over the 32 oscillations that were sampled which each transducer. The number of cycles to sample was selected as a compromise between having enough cycles to get reliable estimates and the changing bathymetry of the sediment bed.

For each transducer the average radial velocity and the average of the square of the velocity fluctuations were computed for each phase. Then, the phase average horizontal velocity $\overline{u}$ and Reynolds stress $\overline{u'v'}$ were obtained using Eqs. (12) and (17), respectively. This was possible due to the high regularity of the LOWST piston motion, which assures that there is no misinterpretation of oscillations irregularities as turbulence. The phase average procedure has been previously used by several authors conducting experiments in oscillatory water tunnels (Hino et al., 1983; Jensen et al., 1989). It is important to note that this regularity cannot be obtained in wave tanks where the random variation of the surface waves may produce velocity fluctuations, and special care should be taken in order to discriminate between these fluctuations and turbulence (see for example Nadaoka et al., 1989; Petti and Longo, 2001; Sakakiyama and Liu, 2001).

After the phase averages were computed, a rectangular Gaussian filter was applied to the profiles in order to remove remaining noise due to the finite number of samples averaged for each flow oscillation phase. The size of the filter (equivalent to 2.5 standard deviations) was 234 ms in time axis and 18 mm in the space axis. The evolution of the mean longitudinal velocity profile over the oscillation cycle is shown in Fig. 3, and the evolution of the Reynolds stress $\overline{u'v'}$ profile over the cycle is shown in Fig. 4. From the figures, it can be seen that the higher values of shear stress near the bed occur just after the flow reversal. At this point it is not possible to evaluate the quality of the data other than qualitatively. Further experiments using a fix bed and smaller roughness could provide results that can be compared with the existing theory and measurements for oscillatory boundary layers.

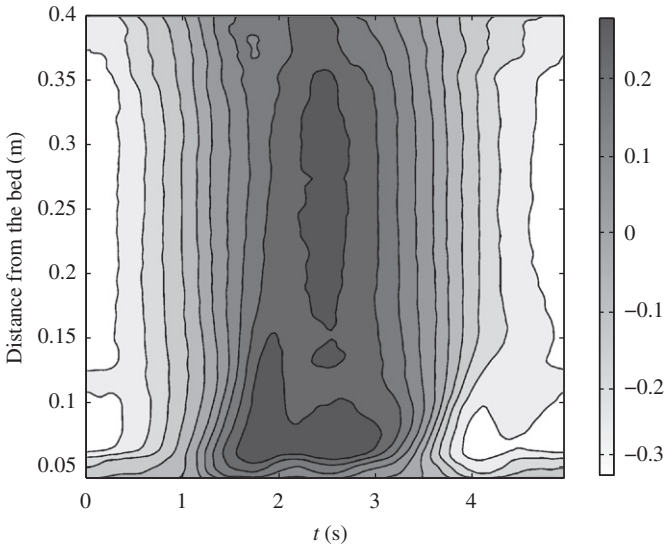

Fig. 3. Contours of longitudinal velocity profiles along the oscillation cycle for an oscillation with $U_{max}=0.3$ m/s and $T=5$ s (velocities in m/s).

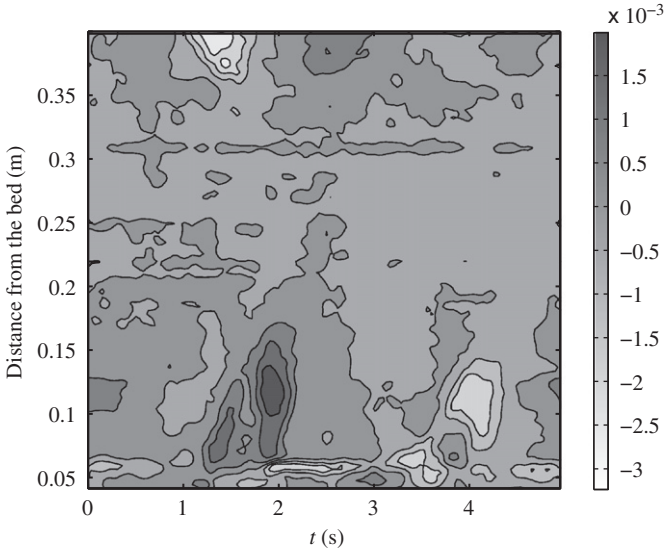

Fig. 4. Contours of Reynolds stress $\overline{u'v'}$ profiles along the oscillation cycle for an oscillation with $U_{max}=0.3$ m/s and $T=5$ s (Reynolds stresses in m^2/s^2).

Please cite this article as: Pedocchi, F., García, M.H., Acoustic measurement of suspended sediment concentration profiles in an oscillatory boundary layer. Continental Shelf Research (2011), doi:10.1016/j.csr.2011.05.013

5.2. Suspended sediment

Previous works have reported problems when trying to apply backscatter-concentration calibrations obtained in calibration facilities to the actual experimental conditions. This problem, as described in Section 4.2, is related to the fact that concentration fluctuations tend to be different in the experiments and in well controlled conditions found in calibration facilities. When the attenuation is large, the nonlinearity in Eq. (28) becomes more important and using an average attenuation tends to overcorrect the measured backscatter amplitudes (Hay, 1991).

The results described herein do not rely on any beforehand calibration. Instead, the calibration was done for each experiment by taking suspended sediment samples continuously during the experiments at two different locations in the water column, 0.1 and 0.3 m above the initial flat sediment bed, using a small peristaltic pump. The location of these sampling points was selected in order to have information both close to and away from the sediment bed. For the usual size of the ripples observed under mild conditions in the LOWST, this locations assure that the bottom point will not be buried by the ripple crests and that at the upper point the suspended sediment concentration does not fluctuate much during the oscillation cycle. The suction samples were taken using two copper pipes with inside diameter of 8.4 mm. The two pipes had their inlets parallel to the flow, and the suction velocity was selected to be three times higher than the maximum mean flow velocity so the trapping efficiency can be considered constant during a given oscillation cycle (Bosman et al., 1987). Under these conditions and for a uniform sand with mean size 250 μm, the trapping efficiency was estimated to be 73% based on the results of Bosman et al. (1987) and Black and Rosenberg (1994). Additionally, Bosman et al. (1987) noted that the trapping efficiency under these conditions is independent of the sediment size. And therefore, the trapping efficiency is also independent of the width of the sediment size-distribution.

For each phase of the oscillation, the backscatter amplitude profiles were inverted using the explicit inversion algorithm (Appendix B). Then, an average profile over the entire flow oscillation cycle was computed, averaging the profiles obtained for each one of the flow oscillation phases. The first transducer channel is located 42 cm above the bed and the value of the concentration at this location is assumed constant over the cycle. The calibration procedure consisted of adjusting the value of the concentration at this first channel. In this way, the mean concentration profiles over the entire oscillation were adjusted to the two point concentrations obtained with the pump (Fig. 5). Since the samples are pumped over several oscillation cycles, the concentration is assumed to be representative of the mean concentration over the oscillation cycle. This calibration is repeated for each experiment in order to obtain the most reliable results for each flow condition.

The Echo Amplitude Signal measured with the central transducer, which is vertically oriented, was used for the backscatter measurements. In addition to the ultrasound measurements, two 3 L water samples at each location were taken. These water samples were filtered and oven-dried in the filters before the dry weight of the sediment contained in the water samples was determined. The two sediment samples at each location were compared and averaged to obtain a final value for the mean suspended sediment concentration at these two vertical locations over the oscillation cycle.

Again, as for the velocity measurements, a rectangular Gaussian filter was applied to the 128 computed mean backscatter profiles in order to reduce some remaining noise before the data inversion. The inverted profiles together with the mean concentration profile over the oscillation cycle after calibration and the two direct concentration measurements are shown in Fig. 5. The evolution of the concentration profile over the cycle is shown in Fig. 6.

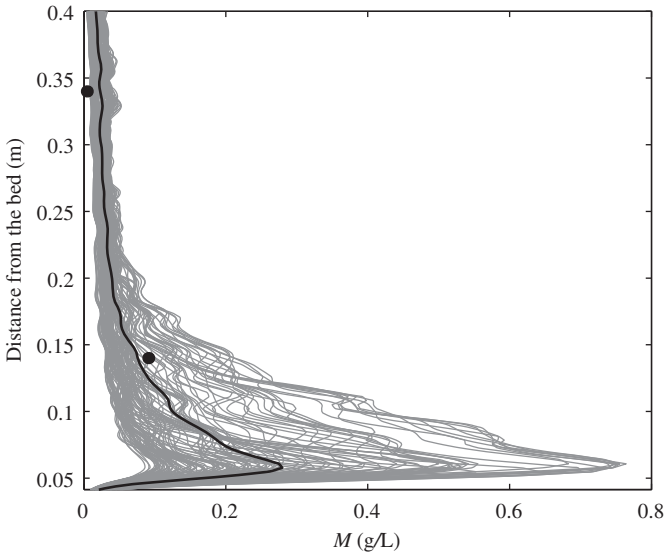

Fig. 5. Inverted suspended sediment concentration profiles for different phases along the oscillation cycle. The bold line corresponds to the mean concentration profile over the cycle that is adjusted to the measured concentration values, indicated by the two dots.

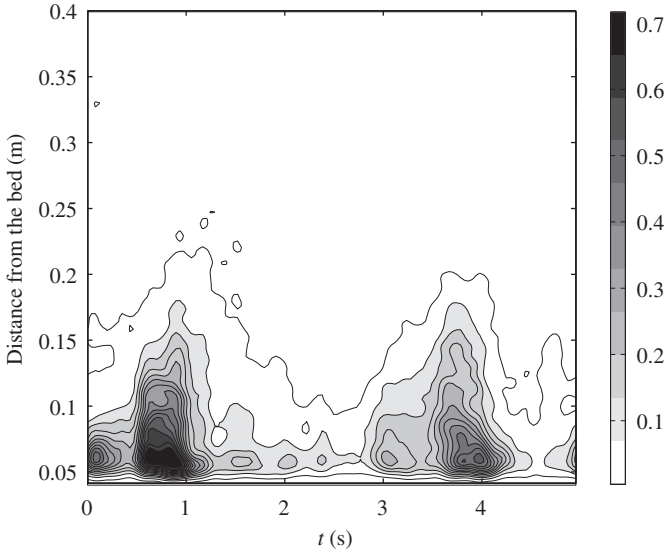

Fig. 6. Contours of suspended sediment concentration profiles along the oscillation cycle for an oscillation with $U_{max}=0.3$ m/s and $T=5$ s, and a sediment bed composed of 250 μm silica sand (concentrations in g/L). Comparing with Figs. 3 and 4, it can be observed that the maximum suspended sediment concentrations are strongly related to the flow reversal.

6. Final remarks

A novel application of a commercially available Ultrasound Velocity Profiler to the study of an oscillatory boundary layer over a movable sediment bed generated inside the Large Oscillatory Water Sediment Tunnel has been presented. Although the use of the UVP for velocity measurements has been presented by other authors, a discussion on the possible bias sources on the estimation of turbulent quantities was not available for the UVP in particular.

The UVP was originally designed only for velocity measurements. However, since the instrument also reports the acoustic

Please cite this article as: Pedocchi, F., García, M.H., Acoustic measurement of suspended sediment concentration profiles in an oscillatory boundary layer. Continental Shelf Research (2011), doi:10.1016/j.csr.2011.05.013

backscatter, the methodology to obtain suspended sediment concentration measurements from the reported echo signal and the errors involved with this technique have been carefully discussed. The capability of measuring both velocity and suspended sediment makes the instrument very appealing for being use in sediment transport studies.

For the experimental configuration used in this particular effort (1 MHz transducers, covering a distance close to a meter), the instrument ability to characterize the turbulence fluctuations $\overline{u'^2}$ and $\overline{v'^2}$ is compromised by the presence of Doppler noise. This may not be the case for flows with higher turbulent energy or for other transducers. In particular, our experience indicates that higher frequency transducers tend to present less noise. Nevertheless, due to the large physical dimensions of the described experiments the use of higher ultrasound frequencies was not possible. The mean velocity is not affected by Doppler noise as long as an adequate number of profiles are averaged. The shear stress $\overline{u'v'}$ can be estimated if a symmetric sensor configuration is used, which cancels out the noise, provided that enough profiles are averaged. However, filtering effects due to the size of the sampling volume may limit the resolution that can be achieved.

Regarding the suspended sediment measurements, the "in situ" calibration was shown to yield good results. For the case of oscillatory flows, this technique allows the study of the suspended sediment profile evolution over the oscillation cycle which would be much more difficult to obtain by direct suction of samples at each phase of the oscillation cycle. Finally, regarding the estimation of the suspended sediment fluctuations, it was shown that, in general, this is only possible for frequencies generally below the turbulence range.

Acknowledgments

The authors would like to thank Juan E. Martin for his help with the preliminary evaluation of the UVP and several suggestions about this work. Thanks to Jeffrey W. Gartner for his comments on an early draft of the manuscript. Also thanks to Blake Landry and David Admiraal for reviewing the manuscript. This work was done under Grant N00014-05-1-0083 from the Coastal Geosciencies Program of the U.S. Office of Naval Research. The LOWST was built and instrumented with the ONR DURIP grants N00014-01-1-0540 and N00014-06-1-0661.

Appendix A. Ultrasound equation summary

The sound propagation speed in fresh water is given by the simplified formula of Lumbbers and Graaff (1998)

$$c = 1405.03 + 4.624T - 3.83 \times 10^{-2}T^2, \tag{A.1}$$

where T is the water temperature in Celsius degrees and c is the sound speed in meters per second.

The form function f in Eq. (20) is given as (Thorne and Hanes, 2002)

$$f = 1.1(1-0.25e^{-4(ka_s-1.4)^2})(1+0.37e^{-(ka_s-2.8)^2/4.84})\left(\frac{1.1(ka_s)^2}{1+1.1(ka_s)^2}\right). \tag{A.2}$$

Also, in Eq. (20), the directivity in the far field $D(\theta)$ for an ideal circular piston transducer with radius a_t is given as (Zemanek, 1971; Hay, 1991)

$$D(\theta) = 2\frac{J_1(ka_t\sin\theta)}{ka_t\sin\theta}, \tag{A.3}$$

where J_1 is the cylindrical Bessel function of first kind. The half-angle $\theta_{-6\ \mathrm{dB}}$, for which the sound pressure decreases to one half of its original value, can therefore then be expressed as

$$\theta_{-6\ \mathrm{dB}} = \arcsin\left(0.25\frac{\lambda}{a_t}\right). \tag{A.4}$$

The voltage amplitude V in Eq. (28) is related to the pressure amplitude P in Eq. (27) by $V = RT_vP$, with R the transducer receive sensitivity, and T_v is the voltage transfer function of the system, which may vary if a varied gain is used. K_t is a constant of the ultrasound system

$$K_t = RT_vp_or_o\frac{0.96}{ka_t}\left(\frac{3}{16}n\lambda\right)^{1/2}. \tag{A.5}$$

Also, in Eq. (28), K_s is a function of the scattering properties of the suspended sediment and it may be expressed as

$$K_s = \frac{f}{\sqrt{a_s\rho_s}}. \tag{A.6}$$

The suspension attenuation $\alpha = \alpha_w + \alpha_s$ is the sum of the water and the sediment attenuation. At atmospheric pressure, the fresh water attenuation α_w is a function of the temperature only (Fisher and Simmons, 1977)

$$\alpha_w = 10^{-15}(55.9-2.37T+4.77\times10^{-2}T^2-3.48\times10^{-4}T^3)F^2, \tag{A.7}$$

with T in Celsius degrees, F in Hertz, and α_w in m^{-1}. The sediment attenuation in Eq. (28) can be computed as

$$\alpha_s = \frac{1}{r}\int_0^r \xi M(r)\,dr, \tag{A.8}$$

with $M(r)$ in $\mathrm{kg/m}^3$, and ξ is the sediment attenuation constant which, for an uniform size suspension, is written as

$$\xi = \frac{3}{4a_s\rho_s}\chi, \tag{A.9}$$

where χ is the normalized total scattering cross-section, and it may be expressed as (Thorne and Hanes, 2002)

$$\chi = \frac{1.1(4/3)0.18(ka_s)^4}{1+1.3(ka_s)^2+(4/3)0.18(ka_s)^4}. \tag{A.10}$$

Finally, in Eq. (28), the function $\psi(r)$ accounts for the departure of the backscattered signal from the spherical spreading in the near field. Near the transducer the amplitude of the pressure field oscillates, while in the far field, the pressure continuously decays. The near field is defined as the region between the transducer and the last pressure maximum. Its extension, if $(\lambda/a_t) \ll 1$, is $r_n = \pi a_t^2/\lambda$ (Zemanek, 1971), and $\psi(r)$ can by evaluated as (Downing et al., 1995)

$$\psi(r) = 1 + \frac{1}{0.43(r/r_n)+0.48(r/r_n)^{3.2}}. \tag{A.11}$$

For the UVP, this correction does not seem to be enough to overcome the distortion effects that are observed in the near field.

Appendix B. Explicit inversion algorithm

The deduction of the explicit method presented Lee and Hanes (1995) starts by taking the logarithm on both sides of Eq. (34)

$$\ln M = 2\ln(r\sqrt{\langle V^2\rangle}) + 2\ln\left(\frac{\psi}{K_sK_t}\right) + 4\left(\alpha_w r + \int_0^r \xi M\,dr\right). \tag{B.1}$$

Then, taking the derivative with respect to r (indicated with primes) on both sides of the equation, results in

$$\frac{M'}{M} = 2\left(\frac{r\sqrt{\langle V^2\rangle}' + \sqrt{\langle V^2\rangle}}{r\sqrt{\langle V^2\rangle}}\right) + 4(\alpha_w + \xi M), \tag{B.2}$$

Please cite this article as: Pedocchi, F., García, M.H., Acoustic measurement of suspended sediment concentration profiles in an oscillatory boundary layer. Continental Shelf Research (2011), doi:10.1016/j.csr.2011.05.013

and rearranging to obtain a Bernoulli type differential equation

$$M' - \left[\left(\frac{r\sqrt{\langle V^2 \rangle}' + \sqrt{\langle V^2 \rangle}}{r\sqrt{\langle V^2 \rangle}} \right) + 4\alpha_w \right] M = 4\xi M^2, \tag{B.3}$$

that has an analytical solution

$$M = \frac{r^2 \langle V^2 \rangle e^{4\alpha_w r}}{\frac{1}{M_l} r_l^2 \langle V^2 \rangle_l e^{4\alpha_w r_l} - 4\xi \int_{r_l}^{r} \langle V^2 \rangle r^2 e^{4\alpha_w r}\, dr}. \tag{B.4}$$

Eq. (B.4) is explicit in M, and if the integral is approximated using trapezoids, it finally takes the discrete form

$$M_n = \frac{r_n^2 \langle V^2 \rangle_n e^{4\alpha_w r_n}}{\frac{1}{M_l} r_l^2 \langle V^2 \rangle_l e^{4\alpha_w r_l} - 2\Delta r \xi \sum_{i=l+1}^{n} (r_i^2 \langle V^2 \rangle_i e^{4\alpha_w r_i} + r_{i-1}^2 \langle V^2 \rangle_{i-1} e^{4\alpha_w r_{i-1}})}. \tag{B.5}$$

Note that the concentration at an initial point M_l should be known in advance. As tested by Lee and Hanes (1995) this inversion algorithm works well if the sediment concentration increases away from the transducer, which is the present case. However, for the case of an uplooking transducer located close to the bed, where the sediment concentration decreases away form the transducer, it was found that this algorithm generally diverges.

References

Admiraal, D., García, M., 2000. Laboratory measurement of suspended sediment concentration using an acoustic concentration profiler (ACP). Experiments in Fluids 28 (2), 116–127.

Bendat, J., Piersol, A., 2000. Random Data: Analysis and Measurement Procedures, third ed. John Wiley & Sons, Inc..

Black, K., Rosenberg, M., 1994. Suspended sand measurements in a turbulent environment: field comparison of optical and pump sampling techniques. Coastal Engineering 24 (1–2), 137–150.

Bosman, J.J., VanDerVelden, E.T.J.M., Hulsbergen, C.H., 1987. Sediment concentration measurements by transverse suction. Coastal Engineering 11 (4), 353–370.

Downing, A., Thorne, P.D., Vincent, C.E., 1995. Backscattering from a suspension in the near field of a piston transducer. Journal of Acoustical Society of America 97 (3), 1614–1620.

Fisher, F.H., Simmons, V.P., 1977. Sound absorption in sea water. Journal of Acoustical Society of America 62 (3), 558–564.

García, C.M., Cantero, M.I., Niño, Y., García, M.H., 2005. Turbulence measurements with acoustic Doppler velocimeters. Journal of Hydraulic Engineering 131 (12), 1062–1073.

Hay, A.E., 1991. Sound scattering from a particle-laden jet. Journal of Acoustical Society of America 90 (4), 2055–2074.

Hino, M., Kashiwayanagi, M., Nakayama, A., Hara, T., 1983. Experiments on the turbulence statistics and the structure of a reciprocating oscillatory flow. Journal of Fluid Mechanics 131, 363–400.

Jensen, B.L., Sumer, B.M., Fredsøe, J., 1989. Turbulent oscillatory boundary layers at high Reynolds numbers. Journal of Fluid Mechanics 206, 265–297.

Lee, T.H., Hanes, D.M., 1995. Direct inversion method to measure the concentration profile of suspended particles using backscattered sound. Journal of Geophysical Research 100 (C2), 2649–2657.

Lemmin, U., Rolland, T., 1997. Acoustic velocity profiler for laboratory and field studies. Journal of Hydraulic Engineering 123 (12), 1089–1098.

Lhermitte, R., Lemmin, U., 1994. Open-channel flow and turbulence measurement by high-resolution Doppler sonar. Journal of Atmospheric and Oceanic Technology 11 (5), 1295–1308.

Lhermitte, R., Serafin, R., 1984. Pulse-to-pulse coherent Doppler sonar signal processing techniques. Journal of Atmospheric and Oceanic Technology 1 (4), 293–308.

Libicki, C., Bedford, K., Lynch, J., 1989. The interpretation and evaluation of a 3-MHz acoustic backscatter device for measuring benthic boundary layer sediment dynamics. Journal of Acoustical Society of America 85 (4), 1501–1511.

Lumbbers, J., Graaff, R., 1998. A simple and accurate formula for the sound velocity in water. Ultrasound Medical Biology 24 (7), 1065–1068.

Mei, R., 1996. Velocity fidelity of flow tracer particles. Experiments in Fluids 22 (1), 1–13.

Merckelbach, L.M., 2006. A model for high-frequency acoustic Doppler current profiler backscatter from suspended sediment in strong currents. Continental Shelf Research 26 (11), 1316–1335.

Met-Flow, 2002. UVP Monitor User's Guide. Met-Flow SA, Lausanne.

Nadaoka, K., Hino, M., Koyano, Y., 1989. Structure of the turbulent flow field under breaking waves in the surf zone. Journal of Fluid Mechanics 204, 359–387.

Nikora, V.I., Goring, D.G., 1998. ADV measurements of turbulence: can we improve their interpretation? Journal of Hydraulic Engineering 124 (6), 630–634.

Pedocchi, F., García, M.H., 2009. Ripple morphology under oscillatory flow. Part II: experiments. Journal of Geophysical Research, Oceans 114 (C12015).

Petti, M., Longo, S., 2001. Turbulence experiments in the swash zone. Coastal Engineering 43 (1), 1–24.

Sakakiyama, T., Liu, P.L.F., 2001. Laboratory experiments for wave motions and turbulence flows in front of a breakwater. Coastal Engineering 44 (2), 117–139.

Thorne, P.D., Hanes, D.M., 2002. A review of acoustic measurement of small-scale sediment processes. Continental Shelf Research 22, 603–632.

Tropea, C., 1983. A note concerning the use of a one-component LDA to measure shear stress terms. Experiments in Fluids 1 (4), 209–210.

Voulgaris, G., Trowbridge, J.H., 1998. Evaluation of the acoustic Doppler velocimeter (ADV) for turbulence measurements. Journal of Atmospheric and Oceanic Technology 15 (1–2), 272–289.

Zemanek, J., 1971. The beam behavior within the nearfield of a vibrating piston. Journal of Acoustical Society of America 49 (1), 181–191.

Please cite this article as: Pedocchi, F., García, M.H., Acoustic measurement of suspended sediment concentration profiles in an oscillatory boundary layer. Continental Shelf Research (2011), doi:10.1016/j.csr.2011.05.013